ACS APPLIED MATERIALS & INTERFACES
Research Article
www.acsami.org

Spatial Atomic Layer Deposition of Zinc Oxide Thin Films

A. Illiberi,[†,*] F. Roozeboom,[†,‡] and P. Poodt[†]

[†]Netherlands Organization for Applied Scientific Research (TNO), PO Box 6235, 5600 HE Eindhoven, The Netherlands
[‡]Department of Applied Physics, Eindhoven University of Technology, PO Box 513, 5600 MB Eindhoven, The Netherlands

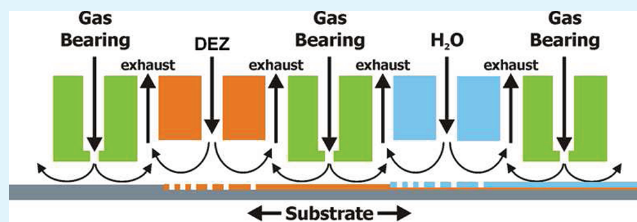

ABSTRACT: Zinc oxide thin films have been deposited at high growth rates (up to ~1 nm/s) by spatial atomic layer deposition technique at atmospheric pressure. Water has been used as oxidant for diethylzinc (DEZ) at deposition temperatures between 75 and 250 °C. The electrical, structural (crystallinity and morphology), and optical properties of the films have been analyzed by using Hall, four-point probe, X-ray diffraction, scanning electron microscopy, spectrophotometry, and photoluminescence, respectively. All the films have *c*-axis (100) preferential orientation, good crystalline quality and high transparency (~ 85%) in the visible range. By varying the DEZ partial pressure, the electrical properties of ZnO can be controlled, ranging from heavily *n*-type conductive (with 4 mOhm.cm resistivity for 250 nm thickness) to insulating. Combining the high deposition rates with a precise control of functional properties (i.e., conductivity and transparency) of the films, the industrially scalable spatial ALD technique can become a disruptive manufacturing method for the ZnO-based industry.

KEYWORDS: *thin films, zinc oxide, atomic layer deposition, deposition rate, industrial process*

■ INTRODUCTION

Zinc oxide (ZnO) has been extensively investigated in recent years because of the increasing number of possible industrial applications.[1,2] Being a wide band gap semiconductor (E_g = 3.4 eV at room temperature), with a large exciton binding energy (60 meV), ZnO is emerging as a prospective material for: ultraviolet light emitters, gas sensors, transparent electronics, surface acoustic wave devices and solar cells.[3,4] The use of ZnO for this variety of different applications requires a nanoscale control of the film structure. Functional properties of ZnO, as conductivity and luminescence, are determined not only by film composition and morphology, but also by intrinsic defects. For example, native donor defects (zinc interstitials, oxygen vacancies, and/or hydrogen) form during the growth of nominally undoped ZnO, making the synthesis of *p*-type ZnO very challenging and, therefore, limiting the use of ZnO in optoelectronic devices.[5] The formation of intrinsic defects during the deposition of ZnO is a kinetically controlled process, which depends on the growth rate, on the parameters used in the growth process (e.g., temperature and oxygen partial pressure) and on the deposition method.[6−8]

Several deposition techniques are used for the growth of ZnO such as: sputtering, pulsed laser deposition, solution process methods, chemical-vapor-deposition (CVD), plasma-enhanced chemical-vapor-deposition (PE-CVD) and atomic layer deposition (ALD).[9−18] The ALD technique is characterized by a time-sequenced introduction of the precursors in the deposition zone, where selective and self-limiting half-reactions occur on the substrate, avoiding parasitic gas phase reactions. Under these conditions, the film growth is completely determined by the kinetic of surface processes. Therefore, ALD enables an accurate control of the incorporation of extrinsic dopants and, possibly, of the formation of intrinsic defects during the film growth. For this reason, ALD has been considered as a promising method for the deposition of doped ZnO films for electrodes of solar cells and organic-light emitting diodes.[19,20] However, conventional ALD is not always compatible with industrial needs, being capable of achieving only growth rates of the order of several hundredths of nm/s.[19] The growth rate is strongly limited by the purge steps between the time-sequenced injection of the precursors, which is typically used to remove excess precursors and reactants.

This drawback of conventional ALD has been overcome by the development of a spatially separated ALD version, where the dosage of the precursors occurs in different zones of the reactor and a moving substrate is sequentially exposed to each of these zones, so that a purge step is no longer needed.[21−23] This concept is illustrated schematically in Figure 1. Spatial ALD combines the advantages of the conventional ALD, i.e., growth of uniform, pinhole free and highly conformal thin films on large area and flexible substrates, with high deposition rates (~nm/s). For this reason, spatial ALD has been proposed as an innovative technique for the growth of thin films in the electronics and solar cell industry.[21,24,25] Recently, high-throughput industrial-scale equipment, based on the spatial ALD technology with double-sided gas bearing, has been successfully commercialized for application in solar passivation.

In this paper, we show that ZnO thin films with controllable electrical properties (from heavily *n*-type to resistive ones) and

Received: September 26, 2011
Accepted: December 15, 2011
Published: December 15, 2011

 © 2011 American Chemical Society

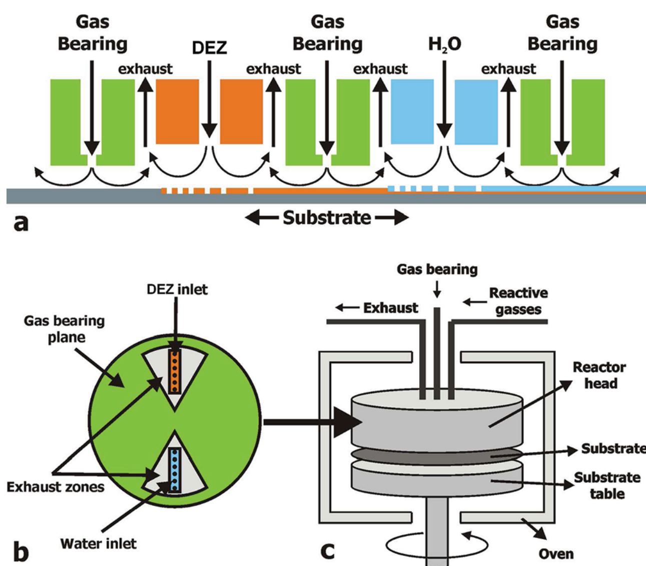

Figure 1. (a) Schematic drawing of the spatial ALD reactor, where the DEZ and water half-reaction zones are separated by gas bearings. By moving the substrate underneath the reactor, the two half-reactions will take place subsequently to form a ZnO monolayer. (b) Schematic drawing of the bottom side of the spatial ALD reactor head, where the DEZ and water half-reaction zones are integrated into inlets surrounded by exhausts zones and gas bearing planes. The colors correspond to Figure.1a. (c) Schematic drawing of the reactor. The reactor head and rotating substrate table with the substrate in between are placed in an oven. The substrate table is rotated by a servo-motor, connected by a drive shaft. The process and waste gas lines are connected to the reactor head through an opening in the top.

high transparency (∼ 85% in the visible range) can be grown at deposition rates up to ∼1 nm/s by means of a spatial ALD technique at atmospheric pressure.

■ EXPERIMENTAL SECTION

A schematic of the spatial-ALD reactor used for the deposition is shown in Figure.1. Different inlets are installed in the circular reactor head, one for each precursor. The substrate is placed on a circular table which rotates underneath the reactor head. During each rotation, the substrate is exposed sequentially to each precursor. Between and around the inlets, shields of inert gas (N_2) separate the precursor flows and seal off the reaction zones, thus making the reactor completely independent of the environment, enabling operation under atmospheric pressure conditions. The entire reactor is installed in a conventional oven, capable of heating up to 400 °C.

For the conditions reported in this paper, diethylzinc [$Zn(C_2H_5)_2$, or DEZ] and water (H_2O) have been used as zinc and oxygen precursors, respectively. Precursors are evaporated from bubblers, by using argon as a carrier gas, and transported to the reactor head through heated lines, to prevent condensation. The DEZ and H_2O bubblers are heated by thermostatic water baths at 32 and 50 °C, respectively, to control the vapor pressure of the precursors. The flow through the water bubbler is kept constant at 1 slm. The flow through the DEZ bubbler is varied as: 0.05, 0.1, 0.15, 0.2, and 0.25 slm, by adjusting the corresponding dilution flows to: 0.95, 0.90, 0.85, 0.80, and 0.75 slm respectively, so that the total flow into the reactor is kept constant at 1 slm. The exposure time of the substrate to both precursors is varied simultaneously by changing the rotation frequency of the substrate, as: 1, 1.7, 3.3, 5, and 10 Hz. ZnO films have been deposited on 15 × 15 cm^2 glass substrates (Schott AF 32, 15 × 15 cm^2) and on *p*-type CZ *c*-Si (100) wafers (for ellipsometry measurements), with pretreatment cleaning by ethanol and subsequent blow drying with nitrogen. The deposition temperature has been varied by setting the oven temperature at: 75, 100, 150, 200, and 250 °C.

The electrical properties and thickness of the films have been determined by using a Phystech RH 2010 Hall effect measurement tool, a Jandel 4-point probe and a Veeco Dektak 8 Advanced Development Profiler, respectively. An X-ray diffractometer with Cu–K_α radiation and a scanning electron microscopy have been used to determine the crystallographic structure and the morphology of the film. Film optical properties have been measured in the near-ultraviolet, visible and near-infrared by a spectrophotometer. Spectroscopic measurements have been performed *ex*-situ by using a J.A. Woollam M2000 rotating compensator ellipsometer in the 300–1000 nm range. For data acquisition and processing, the WVASE software from Woollam was used. The optical constants of the films have been determined by using a Cauchy-like dispersion model in the 500–1000 nm range. The photoluminescence spectra were measured by using Xe lamp excitation with an excitation wavelength of 325 nm at room temperature.

■ RESULTS AND DISCUSSION

The relation between film thickness and number of rotations (i.e., cycles) has been investigated, for a set deposition temperature of 250 °C. As displayed in Figure 2, film thickness increases linearly with the number of rotations indicating that films have been grown by an ALD mode. From the slope of the line in Figure 2, a growth per cycle (GPC) of ∼0.18 nm/cycle is calculated, which is similar to the growth rate reported for ZnO deposited by conventional ALD.[26,27] Growth per cycle of 0.18 nm/cycle, at rotation frequency of 5 Hz, results in a deposition rate of 0.9 nm/s, which is about hundred of times faster than the deposition rate typically achieved by conventional ALD (∼ 0.01 nm/s) and comparable to the growth rate achieved by industrially scalable deposition techniques, as PE-CVD and sputtering.[11,12]

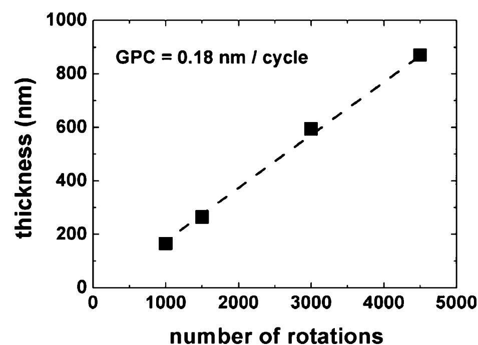

Figure 2. Film thickness as a function of the number of the reactor head rotations (or cycles). The growth per cycle (GPC) has been determined to be 0.18 nm/cycle. Films are deposited at a temperature of 250 °C, DEZ partial pressure of 4.58 mbar, water partial pressure of 116 mbar and a rotation frequency of 5 Hz.

Figure 3 shows the variation of the GPC and refractive index as a function of the deposition temperature. At low deposition temperature, the GPC increases with temperature. In this regime the film growth is controlled by kinetically limited surface reactions, as adsorption/reaction of precursors. With increasing deposition temperature, the GPC becomes independent of the deposition temperature and an ALD process window is reached, where the film growth at atmospheric pressure is limited by the time scale related to the supply of precursors to the substrate and by the mass required for the deposition of each monolayer. A maximum GPC of ∼0.18 nm/cycle is achieved for a deposition temperature of 200 and 250

dx.doi.org/10.1021/am2013097 | ACS Appl. Mater. Interfaces 2012, 4, 268–272

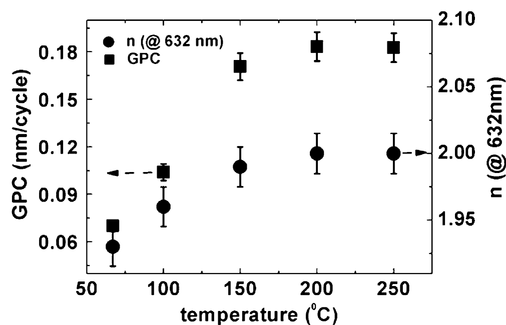

Figure 3. Growth per cycle (GPC, left) and refractive index at 632 nm (n, right) versus deposition temperature. Films are deposited at a rotation frequency of 1.7 Hz with 1500 rotations (i.e., cycles), DEZ partial pressure of 4.58 mbar and water partial pressure of 116 mbar.

°C. Although the growth per cycle of Spatial ALD corresponds to the values reported in literature for the conventional ALD of ZnO, it is achieved at deposition temperatures (200−250 °C) which are higher than for conventional ALD (120−180 °C). According to F.S Nelson et al., the temperature at which the GPC of Spatial ALD reaches the maximum value increases, with respect to the conventional ALD, when decreasing the "purge time", i.e. exposure time of the substrate to the N_2 gas bearing (∼10 s for conventional ALD and ∼0.3 s for the conditions used in this paper at a rotation frequency of 1.7 Hz).[28] The trend of refractive index vs temperature mirrors that of the GPC, initially increasing and then saturating at about 2.0 (at 632 nm), as typically measured for dense ZnO films.[29]

Industrial applications of ZnO require the use of a deposition process with high growth rate, but also with a precise control of the film functional properties (i.e., conductivity and transparency). The dependence of the ZnO conductivity on the film stoichiometry has been extensively investigated in literature, in an attempt to control the formation of intrinsic defects. The stoichiometry of ZnO is typically varied by changing the oxygen and/or zinc partial pressure, during film deposition or annealing.[8,30] In an ALD process, the partial pressure of precursors, together with the exposure time of the substrate (i.e., rotation frequency) to the precursors, determines the GPC. In Figure 4 we show the GPC as a function of the

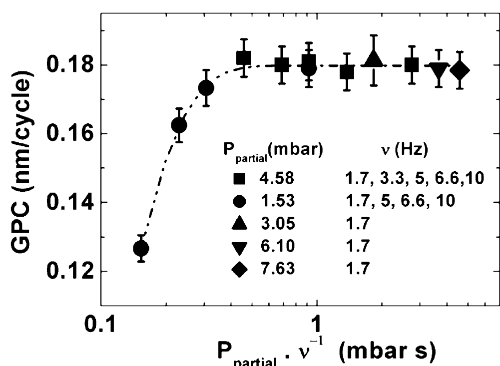

Figure 4. Growth per cycle (GDP) versus the product of DEZ partial pressure and reciprocal rotation frequency of the reactor head. All the films are deposited at a temperature of 250 °C with 1500 rotations (i.e., cycles).

product of the DEZ partial pressure and the reciprocal rotation frequency (ν), for a constant water partial pressure (116 mbar) and a deposition temperature of 250 °C. For very short exposure time and/or DEZ partial pressure (p/ν < 0.4 mbar s), a low GPC is measured, because the mass of DEZ injected into the reactor is less than the mass required to grow a monolayer or the exposure time is shorter than the time scale needed to the supply of precursors to the entire film surface. For p/ν > 0.4 mbar s, GPC reaches the saturation value of ∼0.18 nm/cycle, which corresponds to the self-saturating growth of ZnO, as previously reported.

In the remaining part of this work, we have investigated the structural, electrical and optical properties of ZnO films, deposited with a self-saturated ALD process by varying DEZ partial pressure between (1.53 mbar and 7.63 mbar) at a constant water partial pressure (116 mbar). All the films are deposited at a rotation frequency of 1.7 Hz, with a total number of rotations (i.e., cycles) of 1500, resulting in a film thickness of about 250 nm.

A typical XRD spectrum of ZnO films is shown in Figure.5. Films have a (100) dominant orientation, although other

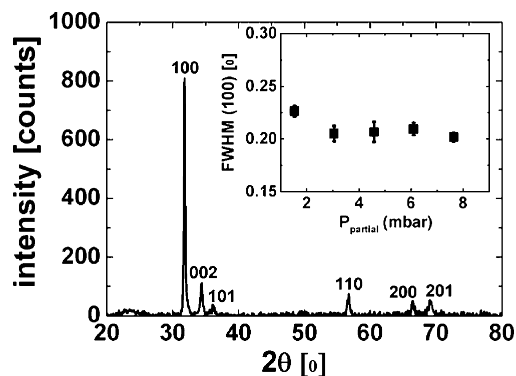

Figure 5. XRD spectrum of ZnO film deposited at 250 °C and DEZ partial pressure of 4.58 mbar. In the inset: FWHM of the (100) peak versus DEZ partial pressure.

orientations are clearly visible. The (100) orientation has been reported as the preferred orientation for ZnO films grown by the Spatial ALD technique, possibly due to the short exposure time of the substrate to the DEZ precursor (∼ 30 ms at 1.7 Hz) and short "purging time" of water (∼0.3 s at 1.7 Hz), which are found to privilege the (100) crystallographic orientation also in conventional ALD of ZnO, instead of the commonly reported (002) orientation.[27,28] The average grain size along the (100) orientation has been calculated from the FWHM of the (100) peak, using the simplified Scherrer formula.[31] As reported in the inset of Figure 5, the FWHM decreases slightly upon raising the DEZ partial pressure from 1.53 to 3.05 mbar, after which it is constant, corresponding to a grain size of 30 nm, thus indicating a good crystalline quality of the films.

In Figure 6, we report the SEM images of ZnO films deposited with a DEZ partial pressure of 1.53, 3.05, and 7.63 mbar, from top to bottom respectively. The top surface of the films present a needle-like structure with a maximum grain size of about 100 nm. The film morphology and the grain size do not change significantly with increasing the DEZ partial pressure.

Although the crystalline structure and morphology of ZnO films do not vary significantly with the DEZ partial pressure, the film resistivity is strongly affected by the DEZ partial pressure, as shown in Figure 7. By increasing the DEZ partial pressure from 1.53 to 4.58 mbar, the film resistivity drops from

dx.doi.org/10.1021/am2013097 | ACS Appl. Mater. Interfaces 2012, 4, 268−272

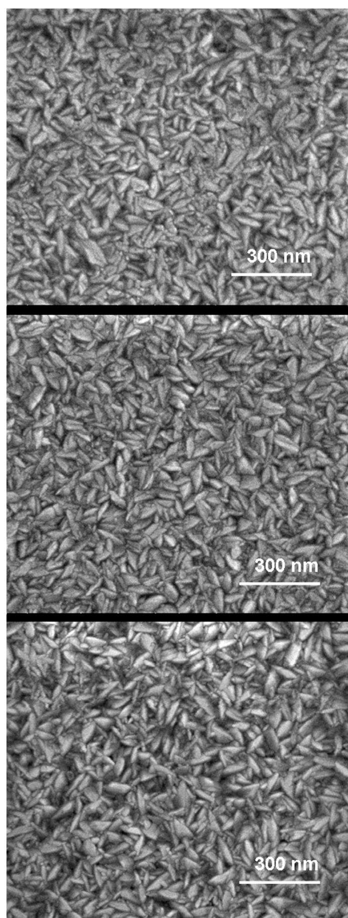

Figure 6. SEM images (top view) of the ZnO films deposited at 250 °C and DEZ partial pressure of 1.53, 3.05, and 7.63 mbar, from top to bottom, respectively.

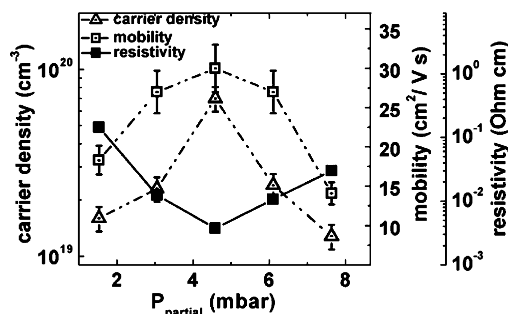

Figure 7. Carrier concentration, mobility, and resistivity of the ZnO films deposited at 250 °C versus DEZ partial pressure. All the films have a thickness of 250 nm.

150 mOhm cm up to a value of about 4 mOhm cm, which belongs to some of the lowest resistivity values reported in literature for intrinsic ZnO films, grown by ALD technique.[16,26] A further increase in DEZ partial pressure, results in the deposition of highly resistive films.

The corresponding values of carrier concentration and mobility are also plotted in Figure 7. The carrier concentration increases with DEZ partial pressure up to an optimum value of 7×10^{19} cm^{-3}, while the mobility reaches a maximum value of 30 cm^2/(V s), possibly due to an increase in the average grain size, as illustrated in Figure 5. With increasing further the DEZ partial pressure, both the carrier concentration and the mobility decrease, possibly due to a self-compensation effect of intrinsic donor defects, by the creation of nonradiative electron recombination centers (such as point defects and dislocations), and/or due to the incorporation of contaminants in films deposited at high DEZ partial pressure.[30]

Optical properties of ZnO films have been investigated by means of spectrophotometer and photoluminescence (PL). The transmission spectrum of ZnO is shown Figure 8. ZnO film exhibits a high optical transmission, reaching a mean value of ~85% in the visible range. Using the standard relation

$$(\alpha h\nu)^2 \approx (h\nu - E_g) \tag{1}$$

we calculated the optical band energy (E_g), which is found to have a systematic blue shift with increasing carrier concentration (n), according to the relation

$$(E_g \approx n^{2/3}) \tag{2}$$

consistent with the Burstein–Moss model (inset in Figure 8).[32]

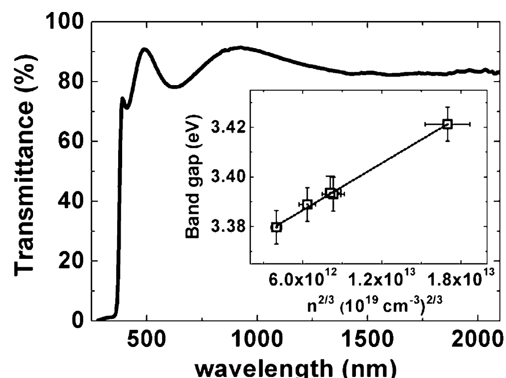

Figure 8. Transmittance spectrum of a typical ZnO film on glass with a thickness of 250 nm, deposited at 250 °C and a DEZ partial pressure of 4.58 mbar. Inset: bandgap as a function of carrier concentration.

PL spectra for films deposited at different DEZ partial pressures are reported in Figure 9. Spectra are characterized by a UV (380–390 nm), a violet/blue emission (400–480 nm)

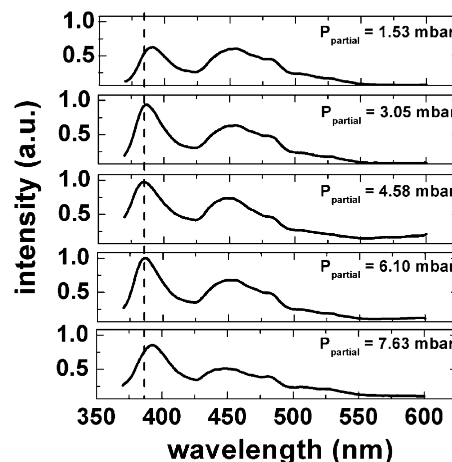

Figure 9. Photoluminescence spectra of ZnO films deposited at 250 °C and at different DEZ partial pressures. All the spectra are normalized to the maximum intensity of the spectrum obtained for a DEZ partial pressure of4.58 mbar. All the films have a thickness of 250 nm.

and a less intense green/yellow emission band (500−600 nm). The UV emission is usually attributed to the band edge transition, to the exciton recombination or to the electron transitions from a band of shallow defects levels (typically located between about 0.02 and 0.2 eV below the edge of the conduction band) to the valence band.[33,34] It has been proposed that these widely ranged donor levels can be ascribed to different types (isolated and extended) of interstitial Zn.[35] Recently, a similar interpretation of the violet/blue emission has been formulated.[36] From a comparison between Figures 7 and 9, we observe that the UV peak blue shifts (from 390 to 380 nm), consistently with the Burstein−Moss effect, and the intensity of the UV emission increases at higher carrier concentration, suggesting a correlation between the increase in DEZ partial pressure (from 1.53 to 4.58 mbar) and the creation of intrinsic defects (interstitial zinc and/or oxygen vacancies), acting as shallow donors.

■ CONCLUDING REMARKS

We have shown that highly conductive and transparent ZnO films can be deposited at high growth rates (up to ∼1 nm/s) by means of spatial-ALD. The electrical properties of the ZnO films, ranging from heavily *n*-type conductive (with 4 mOhm.cm resistivity for 250 nm thickness) to insulating, are controlled by a variation of the DEZ partial pressure. Combining the control of defects-related functional properties (i.e., conductivity and transparency) of ZnO with a high growth rate, the industrially scalable spatial-ALD technique has the potential of becoming a disruptive manufacturing method for the ZnO-based industry.

■ AUTHOR INFORMATION

Corresponding Author

*E-mail: andrea.illiberi@tno.nl.

■ ACKNOWLEDGMENTS

The authors acknowledge E. van Veldhoven (TNO Delft) for the SEM measurements.

■ REFERENCES

(1) Granqvist, C. G. *Sol. Energy Mater. Sol. Cells* **2007**, *91*, 1529.
(2) Klinshirn, C. F.; Meyer, B. K.; Wang, A.; Hoffmann, A.; Geurts, J. *Zinc Oxide: From Fundamental Properties Towards Novel Applications*; Springer Series in Materials Science; Springer: New York, 2010; p 120.
(3) Groenen, R.; Loffler, J.; Sommeling, P. M.; Linden, J. L.; Harmes, E. A. G.; Schropp, R. E. I.; van de Sanden, M. C. M. *Thin Solid Films* **2001**, *392*, 226.
(4) Raniero, L.; Ferreira, I.; Pimentel, A.; Goncalves, A.; Canhola, P.; Fortunato, E.; Martins, R. *Thin Solid Films* **2006**, *511*, 295.
(5) Kobayashi, A.; Sankey, O. F.; Down, J. D. *Phys. Rev. B: Solid State* **1983**, *28*, 946.
(6) Ischenko, V.; Polarz, S.; Grote, D.; Stavarache, V.; Fink, K.; Driess, M. *Adv. Funct. Mater.* **2005**, *15*, 1945−1954.
(7) Cui, J. *J. Phys. Chem. C* **2008**, *112*, 10385−10388.
(8) Tomlins, G. W.; Routbort, J. L.; Mason, T. O. *J. Appl. Phys.* **2000**, *87*, 1.
(9) Hu, J.; Gordon, R. G. *J. Appl. Phys.* **1992**, *71*, 880.
(10) Illiberi, A.; Kniknie, B; van Deelen, J.; Steijvers, H. L. A. H.; Habets, D.; Simons, P. J. P. M.; Janssen, A. C.; Beckers, E. H. A. *Sol. Energy Mater. Sol. Cells* **2011**, *95*, 1955.
(11) Volintiru, I.; Creatore, M.; Kniknie, B. J.; Spee, C. I. M. A.; van de Sanden, M. C. M. *J. Appl. Phys.* **2007**, *102*, 043709.
(12) Sittinger, V.; Ruske, F.; Werner, W.; Szyszka, B.; Rech, B.; Hupkes, J.; Schope, G.; Stiebig, H. *Thin Solid Films* **2006**, *496*, 16.
(13) Matsubara, K.; Fons, P.; Iwata, K.; Yamada, A.; Sakurai, K.; Tampo, H.; Niki, S. *Thin Solid Films* **2003**, *431*, 369.
(14) Major, S.; Banerjee, A.; Chopra, K. L. *Thin Solid Films* **1983**, *108*, 333.
(15) Zhu, M. W.; Gong, J.; Sun, C.; Xia, J. H.; Jiang, X. *J. Appl. Phys.* **2008**, *104*, 073113.
(16) Lujala, V.; Skarp, J.; Tammenmaa, M.; Suntola, T. *Appl. Surf. Sci.* **1984**, *82/83*, 34−40.
(17) Yang, S.; Lin, B. H.; Liu, W. R.; Lin, J.-H.; Chang, C. S.; Hsu, C.-H.; Hsieh, W. F. *Cryst. Growth Des.* **2009**, *9*, 5184.
(18) Alessandri, I.; Zucca, M.; Ferroni, M.; Bontempi, E.; Depero, L. E. *Cryst. Growth Des.* **2009**, *9*, 1258.
(19) Godlewski, M.; Guziewicz, E.; Luka, G.; Krajewski, T.; Lukasiewicz, M.; Wachnicki, L.; Wachnicka, A.; Kopalko, K.; Sarem, A.; Dalati, B. *Thin Solid Films* **2009**, *518*, 1145−1148.
(20) Luka, G.; Stakhira, P.; Cherpak, V.; Volynyuk, D.; Hotra, Z.; Godlewski, M.; Guziewicz, E.; Witkowicz, B.; Kostruba, A. *J. Appl. Phys.* **2010**, *108*, 064518.
(21) Poodt, P.; Lankhorst, A.; Roozeboom, F.; Spee, K.; Maas, D.; Vermeer, A. *Adv. Mater.* **2010**, *22*, 3564.
(22) Suntola, T.; Antson, J. U.S. Patent 4 058 430, Nov. 15, 1977.
(23) Levy, D. H.; Nelson, S. F.; Freeman, D. *J. Disp. Technol.* **2009**, *5*, 484.
(24) Levy, D. H.; Nelson, S. F.; Freeman, D. *J. Disp. Technol.* **2009**, *5*, 12.
(25) Levy, D. H.; Freeman, D.; Nelson, S. F.; Cowdery-Corvan, P. J.; Irving, L. M. *Appl. Phys. Lett.* **2008**, *92*, 192101.
(26) Kim, S. K.; Hwang, C. S.; Park, S. H. K.; Yun, S. J. *Thin Solid Films* **2005**, *478*, 103.
(27) Guziewicz, E.; Kowalik, I. A.; Goglewski, M.; Kopalko, K.; Osinniy, V.; Wojcik, A.; Yatsunenko, S.; Lusakowska, E.; Paszkowicz, W.; Guziewicz, M. *J. Appl. Phys.* **2008**, *103*, 033515.
(28) Nelson, S.F.; Levy, D.H.; Tutt, L.W.; Burberry, M.; , *J. Vac. Sci. Technol., A* **2011**, DOI: 10.1116/1.3670878.
(29) Rowlette, P. C.; Allen, C. G.; Bromley, O. B.; Dubetz, A. E.; Wolden., C. A. *Chem. Vap. Deposition* **2009**, *15*, 15−20.
(30) Ke, L.; Lai, S. C.; Ye, J. D.; Kaixin, V. L.; Chua, S. J. *J. Appl. Phys.* **2010**, *108*, 084502.
(31) Suryanarayana, C.; Grant Norton, M. , *X-ray Diffraction − A Practical Approach*; Plenum Press: New York, 1998.
(32) Burstein, E. *Phys. Rev.* **1954**, *93*, 632.
(33) Rakhshani, A. E.; Bumajdad, A.; Kokaj, J. *Appl. Phys. A: Mater. Sci. Process.* **2007**, *89*, 923−928.
(34) Zhang, D. H.; Xue, Z. Y.; Wang, Q. P. *J. Phys. D: Appl. Phys.* **2002**, *35*, 2837−2840.
(35) Oh, D. C.; Suzuki, T.; Kim, J. J.; Marino, H.; Hanada, T.; Cho, M. W.; Yao., T. *Appl. Phys. Lett.* **2005**, *86*, 032909.
(36) Zeng, H.; Duan, G.; Li, Y.; Yang, S.; Xu, X.; Cai, W. *Adv. Funct. Mater.* **2010**, *20*, 561.